KamLAND: STUDYING NEUTRINO OSCILLATION WITH REACTORS AND MEASURING ANTI-NEUTRINOS FROM THE EARTH*

Michał Patrick Decowski
for the KamLAND Collaboration

Department of Physics, University of California, Berkeley, CA 94720, USA

(Received November 15, 2005)

The KamLAND experiment uses reactor anti-neutrinos to study the solar neutrino oscillation parameters. KamLAND recently updated the reactor neutrino measurement, with five times more statistics than previously reported. The measured spectral distortion in the anti-neutrino spectrum strongly favors neutrino oscillation as the explanation for neutrino disappearance and provides the most accurate value of Δm^2_{12} to date. KamLAND also performed a first observation of geologically produced anti-neutrinos, which can help in understanding the Earth's heat generation and interior composition.

PACS numbers: 14.60.Pq, 26.65.+t, 28.50.Hw, 91.35.Dc

1. Introduction

A large number of reactor anti-neutrino experiments have been conducted in the past 50 years. In 1956, one of the first such experiments, at the Savannah River Reactor Plant, measured first evidence of the anti-neutrino and measured its proton cross section. The original experiments were located only a few meters from the reactor core, the source of anti-neutrinos. In the years since that first experiment, reactor neutrino experiments have steadily increased their baselines, with the goal to ultimately find neutrino disappearance. That goal was reached in 2002, when the KamLAND experiment reported first observation of reactor anti-neutrino disappearance at an average reactor–detector baseline of $\sim$180 km [1].

Nuclear reactors emit electron anti-neutrinos ($\overline{\nu}_e$) isotropically during the decay of neutron-rich radioactive products of the fission process. Without a disappearance mechanism, one expects to measure a $1/R^2$ anti-neutrino

* Presented at the XXIX Mazurian Lakes Conference on Physics August 30–September 6, 2005, Piaski, Poland.

flux decrease with increasing distance R. If neutrinos have mass, however, they may oscillate into flavors undetectable to the detector, leading to an apparent disappearance of electron anti-neutrinos.

Neutrino oscillation arises when the neutrino flavor eigenstates (these are the observable states) are not the same as the neutrino mass eigenstates (the states where neutrinos have definite mass). From LEP experiments it is known that there are three active neutrinos and the oscillation occurs between all three states. However, for reactor experiments considering only two neutrino states is a very good approximation. The survival probability of a $\overline{\nu}_e$ with energy E_ν after traveling a distance L from the reactor is then approximately given by:

$$P(\overline{\nu}_e \to \overline{\nu}_e) = 1 - \sin^2 2\theta \sin^2 \left(1.27 \, \frac{\Delta m^2[\mathrm{eV}^2] \; L[\mathrm{m}]}{E_\nu[\mathrm{MeV}]}\right), \tag{1}$$

where $\Delta m^2 = |m_1^2 - m_2^2|$ is the difference of the mass-squares of the two mass eigenstates that are responsible for generating the oscillation and θ is the mixing angle between the two neutrino mass eigenstates.

The $\overline{\nu}_e$ spectrum emitted by commercial reactors can be calculated with $\sim 2\%$ uncertainty from $\overline{\nu}_e$ spectra and the reactor fission rates for ^{235}U, ^{238}U, ^{239}Pu and ^{241}Pu provided by the power companies operating the reactors. The average reactor $\overline{\nu}_e$ energy is 4 MeV. The low energy of reactor anti-neutrinos make the experiments especially sensitive to low values of Δm^2. In addition, since the oscillation probability function explicitly depends on E_ν, any oscillatory behavior should also manifest itself in a distortion of the neutrino energy spectrum.

Reactors are not the only source of $\overline{\nu}_e$. In the decay of potassium, uranium and thorium in the Earth a substantial, but currently unknown, number of $\overline{\nu}_e$ is also produced. The spectrum of these so-called geo-neutrinos is lower in energy than most of the reactor anti-neutrino spectrum; the geo-neutrino spectrum only extends to $E_{\overline{\nu}_e} = 3.3$ MeV and can, therefore, be suppressed by employing an energy cut.

2. The KamLAND experiment

The most recent large reactor neutrino experiment is the KamLAND experiment in Japan. The experiment searches for neutrino oscillation using a baseline that is two orders of magnitude larger than used in previous reactor experiments. Due to the long baseline, the $\overline{\nu}_e$ flux is significantly decreased relative to earlier experiments, necessitating a much larger detector volume to compensate for the loss in flux. However, the increased volume of the detector also demands more shielding from cosmic backgrounds to avoid dead time, this effectively means that the detector has to be placed deep underground.

KamLAND is situated in the old Kamiokande cavity in a horizontal shaft mine in the Japanese Alps. The site is surrounded by 53 Japanese commercial power reactors, at a flux weighted average distance of 180 km from the reactors. This baseline makes KamLAND sensitive to the neutrino mass-splitting associated with the solar neutrino problem and in particular to the large mixing angle (LMA) solution.

KamLAND consists of a stainless steel sphere of 18 m diameter with 1879 photomultiplier tubes mounted to the inner surface, see Fig. 1. Inside the sphere is a 13 m diameter nylon balloon filled with 1 kton of liquid scintillator. Outside of the balloon, non-scintillating, highly purified oil provides buoyancy for the balloon and acts as a shield against external radiation. The energy resolution of the detector is $6.2\%/\sqrt{E(\mathrm{MeV})}$. Surrounding the detector outside of the stainless steel sphere is a water Cerenkov detector which provides a muon veto counter and acts as shielding from radioactivity in the rock.

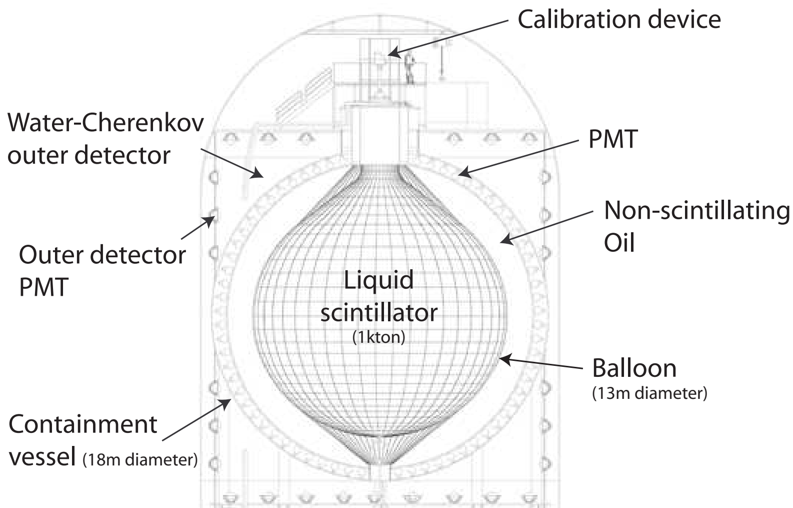

Fig. 1. Sketch of the KamLAND detector.

3. Analysis methodology

Electron anti-neutrinos are detected via inverse β-decay, $\overline{\nu}_e + p \to e^+ + n$, which has a 1.8 MeV $\overline{\nu}_e$ energy threshold. The prompt scintillation light from the e^+ gives an estimate of the incident $\overline{\nu}_e$ energy, $E_{\overline{\nu}_e} = E_{\mathrm{prompt}} + \overline{E}_n + 0.8\,\mathrm{MeV}$, where E_{prompt} is the prompt event energy including the positron kinetic energy and the annihilation energy, and $\overline{E}_n$ is the average neutron recoil energy, which is typically a few tens of keV. The neutron captures on hydrogen $\sim 200\,\mu$s later, giving off a characteristic 2.2 MeV γ ray. This delayed coincidence is a powerful tool for reducing background.

The analysis presented here utilizes the following event selection cuts [2]: (a) a radial fiducial volume cut of 5.5 m; (b) a time difference between the positron and delayed neutron of $0.5\mu\text{s} < \Delta T < 1000\mu\text{s}$; (c) a position difference of $\Delta R < 2\,\text{m}$ between the two events; (d) a prompt event energy of $2.6\,\text{MeV} < E_{\text{prompt}} < 8.5\,\text{MeV}$ and (e) a delayed event energy of $1.8\,\text{MeV} < E_{\text{delayed}} < 2.6\,\text{MeV}$. The prompt energy threshold of 2.6 MeV (corresponding to $E_{\overline{\nu}_e} = 3.4\,\text{MeV}$) significantly cuts backgrounds and avoids the effect of anti-neutrinos from uranium and thorium decaying in the Earth (see Section 5 for a discussion of geo-neutrinos). The efficiency of all cuts is $(89.8 \pm 1.5)\%$. The total systematic uncertainty is 6.5%, where the largest contribution is due to the systematic uncertainty of the fiducial volume. The total live-time of the data presented here for the neutrino oscillation analysis is 515 days [2].

Understanding backgrounds is vital in KamLAND. The background from accidental correlations of radioactive decays in KamLAND is estimated by employing an off-time coincidence window; it is 2.69 ± 0.02 events in the data sample. Fast neutrons coming from muon spallation interactions in the rock outside of KamLAND contribute less than 0.9 background events. Other cosmogenically produced background comes from the beta delayed-neutron emitter ^{9}Li. This background is suppressed by either tracking the preceding muon and vetoing a detector volume in a 3 m radius around the muon track for 2 s or vetoing the entire detector for the same amount of time in case of muon events with a large energy deposition or when the muon could not be tracked reliably. We estimate that the ^{9}Li background contributes 4.8 ± 0.9 events to the data sample.

Finally, the fourth and largest background contribution is an indirect background triggered by α-decay in ^{210}Po. The 5.3 MeV α has a small probability of interacting with ^{13}C in the scintillator (^{13}C has a 1.1% natural abundance in carbon). The subsequent neutron from the $^{13}\text{C}(\alpha, n)^{16}\text{O}$ reaction has a few MeV kinetic energy and will predominantly loose energy through elastic scattering on protons in the scintillator. The quenched proton energy will mostly be below the 2.6 MeV analysis threshold, however, the neutron also has a small probability of inelastically interacting with ^{12}C in the scintillator, emitting a 4.4 MeV γ, or exciting the ^{16}O to the 6 MeV state. The prompt neutron energy loss and the subsequent capture of the neutron makes the signature of these events similar to the $\overline{\nu}_e$ signature. These events contribute 10.3 ± 7.1 events to the total background of 17.8 ± 7.3 events. The observed prompt energy of the (α, n) background is shown in Fig. 2.

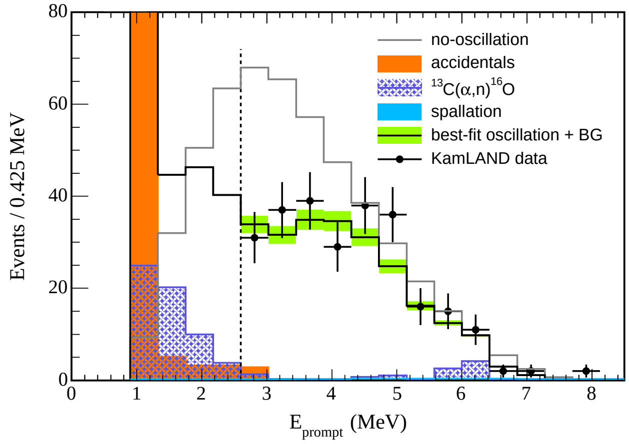

Fig. 2. Prompt event energy spectrum of $\overline{\nu}_e$ candidate events with associated background spectra [2]. The shaded band indicates the systematic error in the best-fit reactor spectrum above 2.6 MeV. Events from the $^{13}\mathrm{C}(\alpha, n)^{16}\mathrm{O}$ reaction are the main background to the measurement.

4. Precision neutrino oscillation parameter measurements

In an exposure of 766 ton-year to reactor $\overline{\nu}_e$ and in the absence of $\overline{\nu}_e$ disappearance, KamLAND expects to observe $365.2 \pm 23.7(\mathrm{syst})$ events above 2.6 MeV. KamLAND observes only 258 $\overline{\nu}_e$ events, confirming $\overline{\nu}_e$ disappearance at the 99.998% significance level. The spectrum of the 258 $\overline{\nu}_e$ candidates, including all backgrounds, is shown in Fig. 2. Performing a two neutrino oscillation analysis, we find a best-fit of $\Delta m^2_{12} = 7.9^{+0.6}_{-0.5} \times 10^{-5}\,\mathrm{eV}^2$ and $\tan^2\theta = 0.46$, with a large uncertainty on $\tan^2\theta$. A statistical analysis of the data [2] finds that the best-fit oscillation parameters have a goodness-of-fit of 11.1%, while the goodness-of-fit of the scaled no-oscillation spectrum where the normalization was fit to the data is only 0.4%.

The left panel of Fig. 3 shows the allowed region contours in $\Delta m^2 - \tan^2\theta$ parameter space derived from $\Delta\chi^2$ values. Superimposed on the shaded KamLAND regions, are the regions determined by solar neutrino flux experiments [3]. KamLAND disfavors the LMA0 region (at $\Delta m^2_{12} \sim 10^{-5}\,\mathrm{eV}^2$) at 97.5% C.L. and also disfavors the LMA II region (at $\Delta m^2_{12} \sim 2 \times 10^{-4}\,\mathrm{eV}^2$) at 98.0 C.L. Larger values of Δm^2_{12} previously allowed by KamLAND are now disfavored at more than 99.73%.

A two neutrino oscillation analysis of a combination of KamLAND data and solar neutrino experiment fluxes (see right panel of Fig. 3) yields the parameters $\Delta m^2_{12} = 7.9^{+0.6}_{-0.5} \times 10^{-5}\,\mathrm{eV}^2$ and $\tan^2\theta = 0.40^{+0.10}_{-0.07}$. With the recently updated full SNO salt analysis [4], a global analysis of solar neutrino fluxes and KamLAND data gives the values $\Delta m^2_{12} = 8.0^{+0.6}_{-0.4} \times 10^{-5}\,\mathrm{eV}^2$ and $\tan^2\theta = 0.45^{+0.09}_{-0.07}$. KamLAND is the only experiment to measure Δm^2 in the solar neutrino sector accurately in the foreseeable future.

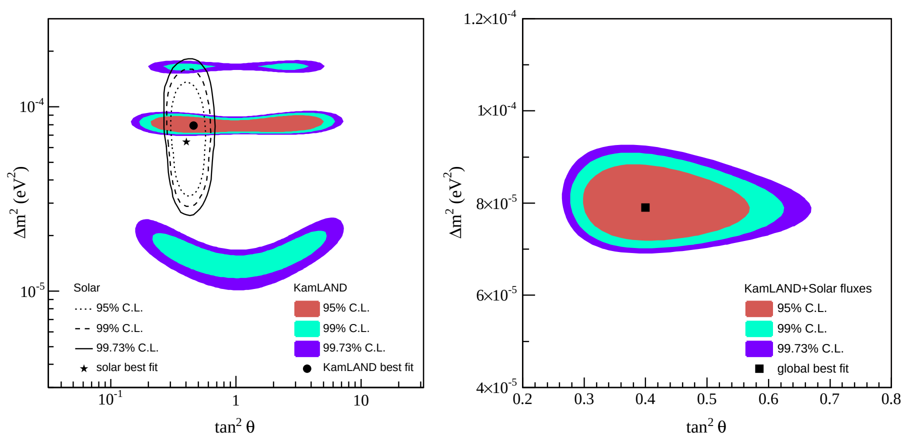

Fig. 3. Left: Neutrino oscillation parameter allowed region from KamLAND anti-neutrino data (shaded regions) and solar neutrino experiments (lines) [3]. Right: Result of a combined two-neutrino oscillation analysis of KamLAND and the observed solar neutrino fluxes under the assumption of CPT invariance.

5. Geologically produced anti-neutrinos

One interesting application of anti-neutrino measurement is the study of geologically produced anti-neutrinos. Although we live on Earth, it is remarkable how little we know or understand about the Earth's internal structure. The deepest borehole that was ever drilled, is less than 20 km deep. Beyond that depth, seismology has revealed that the Earth consists of a layered structure, with a thin core near the surface, a thick mantle in the mid-range and a core in the center of the Earth; these can further be subdivided, see Fig. 4. Lava flows bring material from the upper mantle to the surface. From the analysis of this material it is known that the crust and mantle are mainly composed of silica, with the crust enriched in uranium, thorium and potassium. However, the amount of U, Th and K in the mantle is unknown. More information can be obtained by examining meteorites. One type of meteorite, so-called carbonaceous chondritic meteorites, in particular is considered to be representative of the solar nebula from which the solar system condensed. These meteorites consist mainly of silicates, oxides and sulfides, but also have a high proportion of water and other volatile components, indicating that they have not been heated since formation and are old enough to be characteristic of the solar nebula. For these reasons the chemical composition of carbonaceous chondritic meteorites is often used as a basic ingredient to model Earth's bulk chemical composition. Most importantly for this discussion, these meteorites also contain trace elements of U and Th and while the absolute concentration of these two elements is unknown, the mass ratio Th/U is measured to be between 3.7 and 4.1 [6].

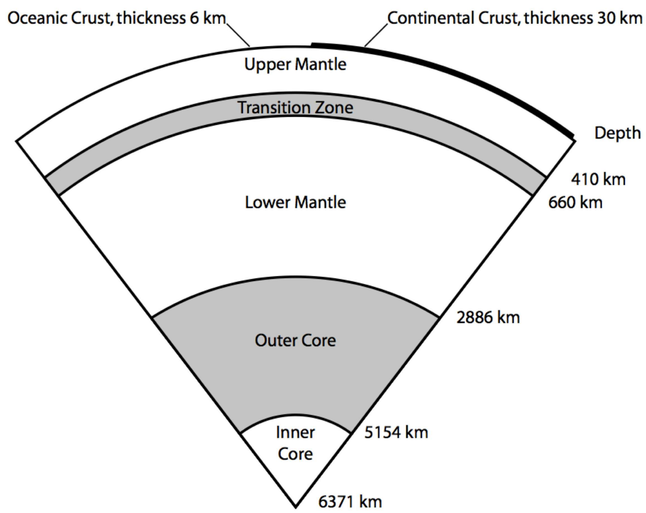

Fig. 4. Radial distribution of the major Earth regions. The older continental crust is much thicker than the relatively young oceanic crust and contains 10–20 times higher concentrations of U, Th and K than the oceanic crust. Taken from [5].

Borehole measurements of the Earth's heat flux show that the Earth produces somewhere between 30–45 TW of heat. Two important sources of heat generation are thought to be the heat released from primordial energy of planetary accretion and latent heat of core solidification. However, it is believed that radiogenically produced heat also plays an important role in the Earth's heat balance. The three main candidates for radiogenic heat production are ^{238}U, ^{232}Th and ^{40}K, they release $98.1\mu\,\mathrm{W\,kg^{-1}}$, $26.4\mu\,\mathrm{W\,kg^{-1}}$ and $0.0035\mu\,\mathrm{W\,kg^{-1}}$ of heat, respectively, [7]. Assuming the bulk of the Earth has the same chemical composition as chondritic meteorites, one geophysical reference model predicts that ^{238}U and ^{232}Th decay each contribute 8 TW of heat and ^{40}K decay contributes 3 TW to the total Earth heat flux [8].

Neutrinos can help in the understanding of the Earth's internal structure and heat generation. ^{40}K, ^{232}Th and ^{238}U produce electron anti-neutrinos in their radioactive decay chains. However, due to the 1.8 MeV inverse beta-decay threshold, KamLAND is only sensitive to anti-neutrinos from ^{238}U and ^{232}Th decay, see Fig. 5.

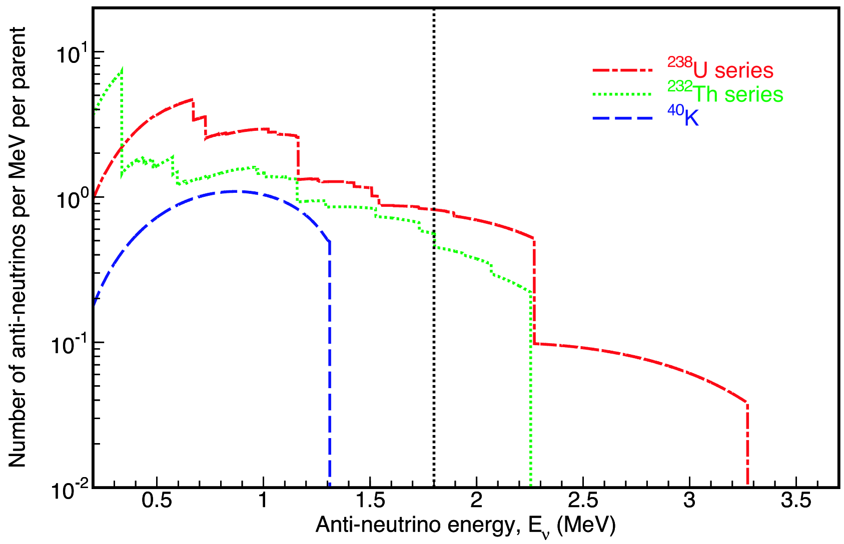

Fig. 5. The expected ^{238}U, ^{232}Th and ^{40}K decay chain electron anti-neutrino spectrum. Due to the 1.8 MeV inverse beta-decay threshold (dotted vertical line), KamLAND is only sensitive to ^{238}U and ^{232}Th anti-neutrinos.

The data presented here is for a total detector livetime of 749.1 days [9]. For this analysis, the prompt energy window was lowered below the reactor energy window presented earlier, it was set to $0.9\,\mathrm{MeV} < E_{\mathrm{prompt}} < 2.6\,\mathrm{MeV}$ ($1.7\,\mathrm{MeV} < E_{\overline{\nu}_e} < 3.4\,\mathrm{MeV}$). Since the accidental background is much higher in this energy window, the radial fiducial volume was reduced to $R < 5$ m; the prompt-delay time correlation was lowered to $\Delta T < 500\,\mu$s and the relative distance cut changed to $\Delta R < 1$ m. Changing these cuts lowered the total efficiency for detecting geo-neutrinos to (68.7 ± 0.7)%.

The main background for this analysis are the reactor anti-neutrinos with 80.4 ± 7.2 events. Scattering of the neutron from the $^{13}\mathrm{C}(\alpha, n)^{16}\mathrm{O}$ reactions off of protons contributes 42 ± 11 events. Other backgrounds come from accidental coincidences, with 2.38 ± 0.01 events and anti-neutrinos from long lived nuclear reactor fission products, with 1.9 ± 0.2 background events. For spallation products, only ^{9}Li β-neutron decays contribute with 0.30 ± 0.05 events. Other backgrounds considered and found to be negligible include spontaneous fission, neutron emitters and correlated decays in the radioactive decay chains and fast neutrons from cosmic ray interactions. The total background for the geo-neutrino analysis is 127 ± 13 events.

After all cuts were applied to the data set, 152 candidate events remained. The anti-neutrino energy distribution is shown in Fig. 6. A "rate only" analysis gives 25^{+19}_{-18} geo-neutrino candidates.

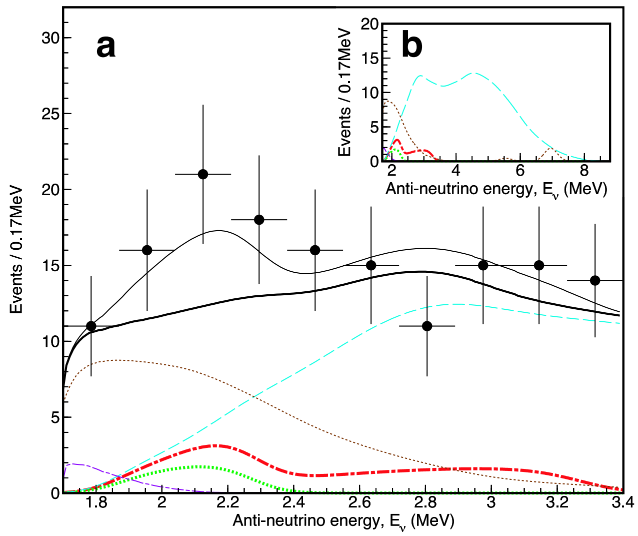

Fig. 6. The measured geo-neutrino energy spectrum. The main panel shows the experimental points and the total expected signal with the geo-neutrino contribution (thin solid line) and without (thick solid line). The expected geo-neutrino signal from ^{238}U (thick dot-dashed line) and ^{232}Th (thick dotted line) assumes 16 TW of radiogenic power. Backgrounds are from reactor anti-neutrinos (thin dashed line), ^{16}C(α,n)^{16}O background (thin dotted line) and random coincidence background (thin dot-dashed line). The inset shows the expected signal extended to higher energies (compare to fig. 2).

An unbinned maximum likelihood analysis was performed to use the spectral shape information to further study the number of observed ^{238}U and ^{232}Th anti-neutrinos. The left panel of Fig. 7 shows the confidence intervals for the total number of geo-neutrinos when floating the Th/U mass ratio. The best-fit point favors 3 geo-neutrinos from ^{238}U decay and 18 from ^{232}Th decay. The right panel of Fig. 7 shows the $\Delta\chi^2$ as a function of the total number of geo-neutrinos while keeping the Th/U mass ratio fixed at 3.9, as determined from chondritic meteorites. The 90% confidence interval for the number of geo-neutrinos is 4.5 to 54.2 events. The central value of 28.0 is consistent with the "rate only" analysis. The 99% confidence upper limit on the total number of detected ^{238}U and ^{232}Th geo-neutrinos is $1.45 \times 10^{-30}\,\overline{\nu}_e$ per target proton per year, corresponding to a total flux at KamLAND of $1.62 \times 10^{7}\,\mathrm{cm}^{-2}\mathrm{s}^{-1}$. This corresponds to an upper limit on the radiogenic power from U and Th decay of between 60 TW and 160 TW, depending on the geological reference model. Since the total heat from the Earth is known to be between 30 and 45 TW, this measurement does not yet usefully constrain the contribution of radiogenic power to the total power.

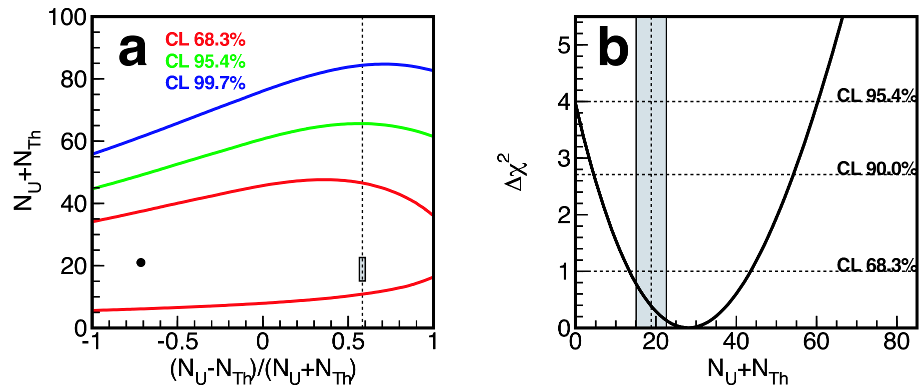

Fig. 7. Left: Confidence regions for the number of detected geo-neutrinos. The small shaded area represents the prediction from a geophysical reference model that assumes that U and Th produce 16 TW of radiogenic power. The vertical dashed line represents the Th/U mass ratio of 3.9. The dot shows the best-fit point. Right: The $\Delta\chi^2$ fit, fixing the Th/U mass ratio to 3.9 (follows the dashed line in the left panel). The 90% confidence interval for the total number of detected geo-neutrinos is 4.5 to 54.2.

6. Conclusion and future outlook

The updated KamLAND neutrino oscillation results have confirmed reactor neutrino disappearance at 99.998% statistical significance. The observed energy spectrum disagrees with the expected spectral shape in the absence of neutrino oscillation at 99.6% significance and prefers the distortion expected from neutrino oscillation. The statistical and systematic uncertainties of the neutrino oscillation rate measurement are now comparable. Current experimental efforts concentrate on reducing the systematic uncertainties. In addition, the KamLAND experiment provided the first observation of a geo-neutrino signal. However, the signal-to-background in the measurement is still too low to meaningfully constrain the amount of radiogenically produced heat in the Earth's interior.

KamLAND is presently embarking on a major new effort to purify the liquid scintillator. This will allow lowering the detector threshold to observe solar ^{7}Be neutrinos through electron scattering in the detector. The purification will also be beneficial for the reactor and geo-neutrino measurements, since this will lower the $^{13}C(\alpha,n)^{16}O$ background and dramatically improve the signal-to-background. The solar neutrino phase of KamLAND is expected to start early 2007.

REFERENCES

[1] K. Eguchi *et al.*, KamLAND Collaboration, *Phys. Rev. Lett.* **90**, 021802 (2003).
[2] T. Araki *et al.*, KamLAND Collaboration, *Phys. Rev. Lett.* **94**, 081801 (2005).
[3] S.N. Ahmed *et al.*, SNO Collaboration, *Phys. Rev. Lett.* **92**, 181301 (2004).
[4] B. Aharmim *et al.*, SNO Collaboration, `nucl-ex/0502021`.
[5] N.R. Tolich, Experimental Study of Terrestrial Electron Anti-Neutrinos with KamLAND, Stanford University 2005.
[6] A. Rocholl, K.P. Jochum, *Earth Planet. Sci. Lett.* **117**, 265 (1993).
[7] G. Schubert, D.L. Turcotte, P. Olson, *Mantle Convection in the Earth and Planets*, Cambridge univercity Press 2001, p. 940.
[8] S. Enomoto, E. Ohtani, K. Inoue, A. Suzuki, `hep-ph/0508049`.
[9] T. Araki *et al.*, KamLAND Collaboration, *Nature* **436**, 499 (2005).